第 35 卷第 2 期
2019 年 2 月

无 机 化 学 学 报
CHINESE JOURNAL OF INORGANIC CHEMISTRY

Vol.35 No.2
337-343

顺、反-1,2-环己二胺对有机–无机杂化锑碘异构体的影响

梁志文 陈晓柔 于 慧 魏振宏* 张秀秀 蔡 琥*
(南昌大学化学学院,南昌 330031)

摘要:在浓氢碘酸水溶液中,顺式和反式-1,2-环己二胺 (DAC) 分别与三碘化锑反应得到 2 种有机–无机杂化异构体(*cis*-1,2-$DACH_2$)$[SbI_5]\cdot H_2O$ (**1**)和{(*trans*-1,2-$DACH_2$)$[SbI_5]\cdot H_2O\}_n$ (**2**)。X 射线单晶衍射表明化合物 **1** 中的无机成分是由 2 个$[SbI_6]$八面体通过共 I-I 边形成的二聚体$[Sb_2I_{10}]$,而化合物 **2** 中的无机部分是$[SbI_6]$八面体通过共享顶点形成的一维锯齿链。此外,利用紫外-可见光谱、荧光光谱和密度泛函理论对化合物 **1** 和 **2** 进行了比较研究。

关键词:1,2-环己二胺;碘化锑;顺反构型;有机无机杂化;晶体结构
中图分类号:O614.53+1 **文献标识码**:A **文章编号**:1001-4861(2019)02-0337-07
DOI:10.11862/CJIC.2019.027

Influences of *cis*-, *trans*-1,2-Cyclohexanediamine Configurations on Iodoantimonate Organic-Inorganic Hybrid Isomers

LIANG Zhi-Wen CHEN Xiao-Rou YU Hui WEI Zhen-Hong* ZHANG Xiu-Xiu CAI Hu*
(*College of Chemistry, Nanchang University, Nanchang* 330031, *China*)

Abstract: Reactions of *cis*- and *trans*-1,2-cyclohexanediamine (DAC) with antimony iodide in concentrated HI aqueous solution afforded two organic-inorganic hybrid isomers (*cis*-1,2-$DACH_2$)$[SbI_5]\cdot H_2O$ (**1**) and {(*trans*-1,2-$DACH_2$)$[SbI_5]\cdot H_2O\}_n$ (**2**), respectively. The single-crystal X-ray diffraction revealed that the inorganic component in compound **1** is a dimer $[Sb_2I_{10}]$ built up from two $[SbI_6]$ octahedra by sharing I-I edge, and that in compound **2** is a zigzag chain constructed with corner-sharing octahedral $[SbI_6]$ units. In addition, both compounds have been investigated and compared by UV-Vis, fluorescent spectra, and DFT calculation. CCDC: 1818719, **1**; 1818718, **2**.

Keywords: 1,2-cyclohexanediamine; antimony iodide; cis- and trans-configuration; organic-inorganic hybrid; crystal structure

0 Introduction

During the past decades, organic-inorganic hybrid compounds have received considerable attention due to their opportunity to combine useful properties of both components[1-3], in which the inorganic component supplies the features of adjustable mechanical composition, large polarity, good optoelectronic properties, thermal stability and electron mobility; and the organic component usually acts as a structure-directing agent and greatly affects the structure of the inorganic part, as well as balances the charge from the inorganic component.

As regards the metal-halide anions, an extensive work has been devoted to the semiconducting metal halide anions (Sn, Pb, Bi, Sb) because the semiconductor metals have an important application in photovoltaic cells because they have suitable band gap width, high light absorption coefficient, the equilibrium electron hole injection distance, and electronic

收稿日期:2018-08-07。收修改稿日期:2018-11-28。
国家自然科学基金(No.21571094,21661021,21865015)和江西省科技厅项目(No.20161BAB203073)资助。
*通信联系人。E-mail:weizh@ncu.edu.cn

mobility characteristics[4-11]. On the other hand, it has been demonstrated that the organic amines as popular templates with tunable size, charge and shape can have a great effect on the final structures and properties of hybrids[12-13]. Most popularly used organic amine cations incorporated in hybrids are either alkylammonium[14-15] or single ring aromatic ammonium cations[16]. As have been already pointed out, the skeleton of diammonium cations is the key to the formation of novel inorganic structures[17-19].

1,2-Cyclohexanediamine (DAC) is an extraordinary interesting molecule because it displays two different stable *cis*- and *trans*-boat configurations as shown in Scheme 1[20-22]. Not only its adjacent two primary amines may have a synergistic effect on the finial structure, but also the *cis*- and *trans*-1,2-cyclohexanediamines can react with the semiconducting metal halide to give different structures of organic-inorganic hybrid compounds, which will help to lay a solid foundation for the following structure-property researches[23-27].

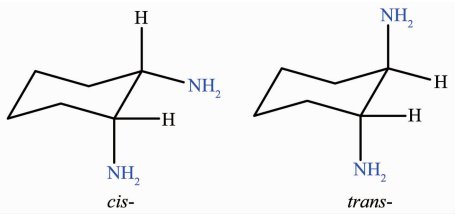

Scheme 1 *cis*- and *trans*-configurations of 1,2-cyclohexanediamine

So, we prepared two organic-inorganic hybrid isomers (*cis*-1,2-DACH$_2$)[SbI$_5$]·H$_2$O (**1**) and {(*trans*-1,2-DACH$_2$)[SbI$_5$]·H$_2$O}$_n$ (**2**) by reactions of *cis*- and *trans*-1,2-DAC with semiconducting metal halide iodoantimonate(Ⅲ), respectively. Herein, we report the syntheses, characterizations, fluorescent properties and DFT calculation of compounds **1** and **2**.

1 Experimental

1.1 Instruments and materials

The starting materials antimony triiodide (SbI$_3$), *trans*-/*cis*-1,2-DAC and the concentrated hydriodic acid (HI) are commercially available and were used as received. Powder X-ray diffraction data of the samples were recorded on an X-ray powder diffractometer (Beijing Persee Instrument Co., Ltd. XD-3) with Cu $K\alpha$ radiation (λ=0.154 06 nm) operating at 40 kV and 15 mA in a range of 5.00°~55.00° (2θ). The elemental analysis of C, H and N were determined using a Vario EL Ⅲ elemental analyzer. The FT-IR spectra were recorded in a range of 4 000~400 cm^{-1} with a Nicolet 5700 Spectrometer using KBr pellets. The UV-Vis spectra were measured at room temperature using a Perkin-Elmer Lambda 900 spectrophotometer. The photoluminescence spectra were conducted on a Hitachi F-7000 fluorescence spectrometer. The DFT calculation of **1** and **2** were performed at the B3LYP level of theory as implemented in the Gaussian 03 program package.

1.2 Synthesis

1.2.1 Compound **1**

To a solution of SbI$_3$ (0.501 6 g, 1.0 mmol) in 10 mL HI aqueous solution (47%), *cis*-1,2-DAC (0.222 1 g, 2.0 mmol) in 5 mL HI solution (47%) was added and the mixture was heated to 90 ℃ and kept stirring for half an hour. After slowly cooling down to room temperature, the mixture gave orange block crystals of **1**, which were filtered and dried under vacuum. Yield: 0.614 0 g, 68%. Anal. Calcd. for C$_6$H$_{18}$N$_2$OSbI$_5$(%): C, 8.09; H, 2.04; N, 3.15. Found(%): C, 8.21; H, 2.02; N, 3.46. IR(KBr, cm^{-1}): 3 437(s), 3 018(s), 2 933(s), 2 866(s), 1 622(m), 1 581(s), 1 561(s), 1 500(s), 1 459(s), 1 388(w), 1 348(w), 1 317(w), 1 266(w), 1 236(w), 1 185(w), 1 155(w), 1 107(w), 1 087(w), 1 036(w), 1 016(w), 955(w), 890(w), 853(w), 806(w), 752(w), 674(w), 613(w), 566(w), 494(w), 423(w).

1.2.2 Compound **2**

The similar procedures for synthesis of compound **1** based on *trans*-1,2-DAC (0.223 1 g, 2.0 mmol) and SbI$_3$ (0.502 3 g, 1.0 mmol) in the concentrated HI aqueous solution gave orange block crystals of **2**. Yield: 0.658 7 g, 74%. Anal. Calcd for C$_6$H$_{18}$N$_2$OSbI$_5$ (%): C, 8.09; H, 2.04; N, 3.15. Found(%): C, 8.23; H, 1.89; N, 2.34. IR (KBr, cm^{-1}): 3 561 (m), 3 494(m), 3 066(m), 2 989(s), 2 942(s), 2 866(s), 1 625(w), 1 586(s), 1 544(m), 1 502(m), 1 477(s), 1 441(m), 1 388(w), 1 366(w), 1 354(w), 1 317(w), 1 277(w), 1 261(w),

1 237(w), 1 205(w), 1 175(w), 1 130(w), 1 079(w), 1 061(m), 1 023(w), 1 006(w), 998(m), 930(w), 898(w), 874(w), 837(w), 767(w), 507(w), 434(w).

1.3 X-ray crystallography

Diffraction data of two block single crystals with dimensions of 0.20 mm×0.18 mm×0.15 mm for **1** and 0.25 mm×0.20 mm×0.15 mm for **2** were collected on a Bruker SMART CCD area detector diffractometer with graphite monochromated Mo $K\alpha$ radiation (λ= 0.071 073 nm). The crystal structures were solved by direct methods using SHELXSL-97. Non-hydrogen atoms were first refined isotropically followed by anisotropic refinement by full matrix least-squares calculations based on F^2 (SHELXL-97)[28]. Hydrogen atoms on carbon and nitrogen atoms were placed in idealized positions and treated as riding atoms. While hydrogen atoms on water were first located in the difference Fourier maps then positioned geometrically and allowed to ride on their respective parent atoms. Crystal data and structure refinement results of compounds **1** and **2** were summarized in Table 1.

CCDC: 1818719, **1**; 1818718, **2**.

Table 1　Crystallographic data for compounds 1 and 2

Compound	1	2
Formula	$C_6H_{18}N_2OSbI_5$	$C_6H_{18}N_2OSbI_5$
Formula weight	890.48	890.48
Crystal system	Monoclinic	Monoclinic
Space group	$P2_1/c$	$P2_1/c$
a / nm	1.131 26(12)	1.209 0(6)
b / nm	0.824 53(9)	0.838 8(4)
c / nm	2.076 9(2)	1.902 2(9)
β / (°)	98.179(2)	94.333(6)
V / nm^3	1.917 5(4)	1.923 5(16)
Z	4	4
D_c / (g·cm^{-3})	3.085	3.075
F(000)	1 568	1 568
θ_{max} / (°)	27.51	24.99
μ(Mo $K\alpha$) / mm^{-1}	9.475	9.446
Total reflection	11 031	12 715
Unique reflection	4 327 (R_{int}=0.046 1)	3 382 (R_{int}=0.035 5)
Variable	142	140
R_1, wR_2 [$I>2\sigma(I)$]	0.038 3, 0.099 4	0.029 4, 0.070 0
R_1, wR_2 (all data)	0.047 1, 0.106 2	0.035 6, 0.072 3
GOF	1.028	1.083

2 Results and discussion

2.1 Synthesis and characterization

The phase purities of **1** and **2** were verified using the powder X-ray diffraction (PXRD) patterns which matched very well with the simulated ones in terms of the single-crystal X-ray data as shown in Fig.1. TG analysis showed that compounds **1** and **2** have similar curves, both firstly lost their crystalline water at a range of 25~120 ℃, then completely decomposed their whole skeletons at a range of 270~350 ℃ (Fig.2).

2.2 Structure comparison

Compounds **1** and **2** are isomers, both crystallize in the monoclinic system with $P2_1/c$ space group. In their asymmetric units, both have a $[SbI_5]^{2-}$ anion, a protonated 1,2-cyclohexanediamine cations (1,2-$DACH_2^{2+}$) and a solvated water. It can be seen from Fig.3 that the *cis*- and *trans*-1,2-$DACH_2^{2+}$ keep their original configurations after reactions with SbI_3.

In compound **1**, two $[SbI_6]$ octahedra are first

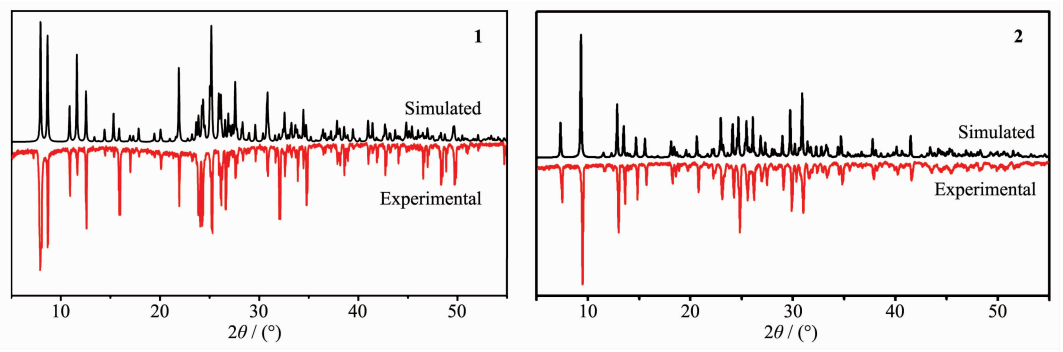

Fig.1 Powder X-ray diffraction patterns of compounds **1** and **2**

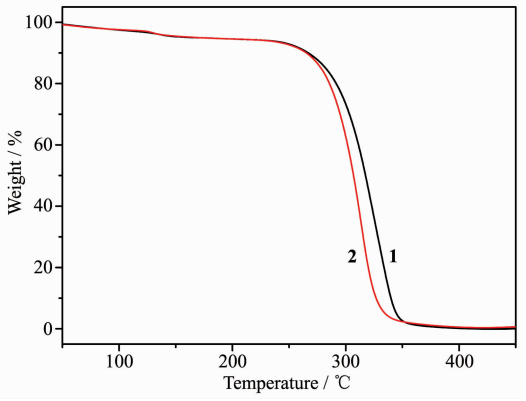

Fig.2 TG curves of compounds **1** and **2**

constructed into a dimer $[Sb_2I_{10}]$ by sharing with the I-I edge. In the dimer, there is a symmetric center locating at the middle of Sb(1)⋯Sb(1A) bond. The crystallographically independent antimony atom is coordinated by six I atoms in a significantly distorted octahedral coordination environment with bond lengths ranging from 0.282 40(6) to 0.329 49(7) nm and the maximum bond angle I(4)-Sb(1)-I(3) of 175.500(18)° (Table 2), consistent with those found in other halogenoantimonate(Ⅲ)[29-30]. On the other side, the *cis*-1,2-DACH$_2^{2+}$ works as a bridge connecting the $[Sb_2I_{10}]$

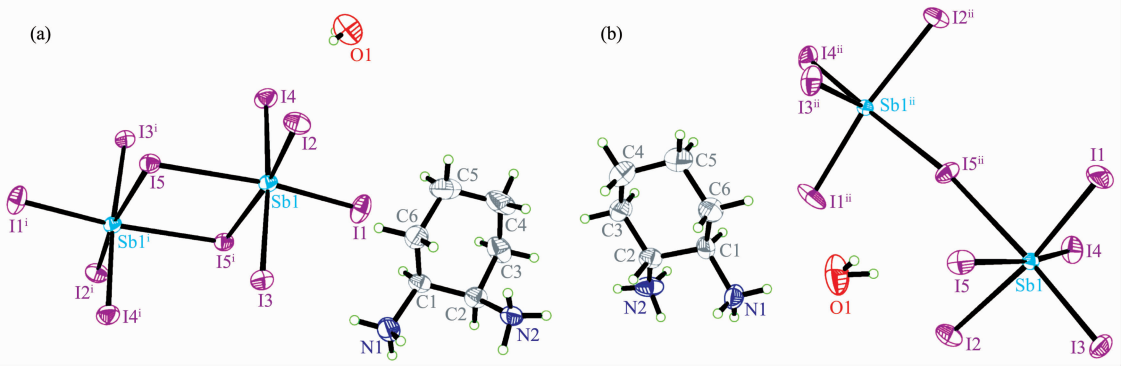

Displacement ellipsoids probability level: 50%; Symmetry codes: [i] 2–*x*, 2–*y*, –*z* for 1; [ii] 3.5–*x*, –0.5+*y*, –0.5–*z* for **2**

Fig.3 Asymmetric units of compounds **1** (a) and **2** (b)

Table 2 Selected bond lengths (nm) and angles (°) for compounds 1 and 2

1					
Sb(1)-I(1)	0.282 40(6)	Sb(1)-I(3)	0.311 71(6)	Sb(1)-I(5)	0.329 49(7)
Sb(1)-I(2)	0.284 29(6)	Sb(1)-I(4)	0.294 36(6)		
I(4)-Sb(1)-I(3)	175.500(18)	I(2)-Sb(1)-I(4)	90.843(19)	I(2)-Sb(1)-I(5)	90.070(16)
I(1)-Sb(1)-I(5)	171.688(20)	I(1)-Sb(1)-I(3)	91.200(18)	I(3)-Sb(1)-I(5)	87.571(15)
I(1)-Sb(1)-I(2)	98.12(2)	I(2)-Sb(1)-I(3)	88.848(18)		
I(1)-Sb(1)-I(4)	93.288(19)	I(4)-Sb(1)-I(5)	87.938(16)		
2					
Sb(1)-I(1)	0.292 64(14)	Sb(1)-I(3)	0.280 92(11)	Sb(1)-I(5)	0.322 64(12)
Sb(1)-I(2)	0.314 19(16)	Sb(1)-I(4)	0.283 42(11)		

Continued Table 2

I(1)-Sb(1)-I(2)	172.01(2)	I(4)-Sb(1)-I(1)	93.27(3)	I(2)-Sb(1)-I(5)	88.06(2)
I(4)-Sb(1)-I(5)	171.127(19)	I(3)-Sb(1)-I(2)	93.51(2)	I(1)-Sb(1)-I(5)	87.12(3)
I(3)-Sb(1)-I(4)	96.52(4)	I(3)-Sb(1)-I(5)	92.31(4)		
I(3)-Sb(1)-I(1)	93.05(2)	I(4)-Sb(1)-I(2)	90.51(2)		

dimers by hydrogen bonds N–H⋯I along *b* direction to form a chain, and the solvated water is linked to the chain by the N–H⋯O hydrogen bond(Fig.4).

While, in compound **2**, the $[SbI_6]^{2-}$ ions are bridged by I5 atom to form a one-dimensional chain along *b* direction, and the *trans*-$DACH_2^{2+}$ ions are connected to the anionic chain by hydrogen bonds in addition to the ionic bond between them. As shown in Table 2, the Sb-I distances, ranging from 0.280 92(11) to 0.322 64(12) nm for the terminal iodine atoms and from 0.283 42(11) to 0.314 19(16) nm for the bridging iodine ones, closely agree with those observed in other zigzag chain structures[31-32]. The *trans*-$DACH_2^{2+}$ and solvated water act as two connecting-points tying together the one-dimensional strands into two-dimensional layered step-like structure by hydrogen bonds(Fig.5).

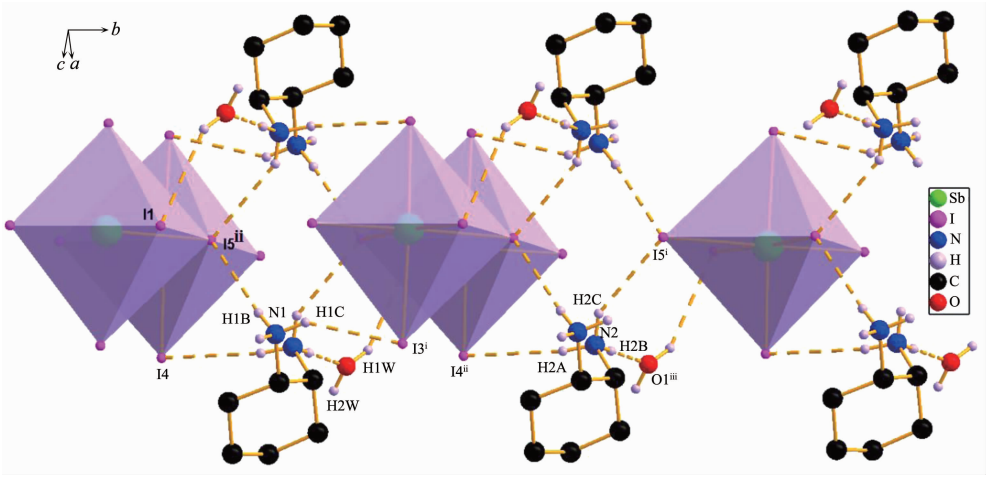

Symmetry codes: [i] 2–*x*, 1/2+*y*, 1/2–*z*, [ii] *x*, 3/2–*y*, 1/2+*z*, [iii] 1–*x*, 1/2+*y*, 1/2–*z*

Fig.4　Anionic dimers $[Sb_2I_{10}]^{2-}$ connecting the *cis*-$DACH_2^{2+}$ cations by hydrogen bonds

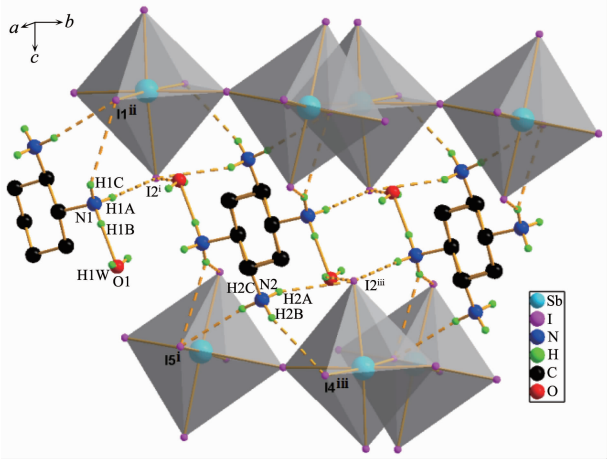

Symmetry codes: [i] 3–*x*, 2–*y*, –*z*, [ii] *x*, 3/2–*y*, 1/2+*z*, [iii] 3–*x*, 1–*y*, –*z*

Fig.5　*trans*-$DACH_2^{2+}$ cations connected to the 1D chain by hydrogen bonds

2.3 Absorption and fluorescent spectra

The room temperature absorptions of compounds **1** and **2** showed very similar curves as shown in Fig.6. In the absorption spectrum of compound **1**, there were three obviously peaks at 235, 362 and 429 nm, which can be attributed to the charge transfer transitions in the ligand, between the organic and inorganic layers, and within the inorganic layers. This is because the organic-inorganic hybrid is a type of semiconductor quantum well structure, typically with small band gap inorganic sheets (carrier) alternating with larger band gap organic layer (well)[33]. Compared with compound **1**, the corresponding peaks in compound **2** were located at 245, 348 and 499 nm which have red shifts, consistent with the rule that the energy gap decreases as the dimensionality increases. The solid fluorescent spectra of compounds **1** and **2** are showed in Fig.7. At the excitation wavelength of 365 nm, compounds **1** and **2** exhibited the emission peaks at 566 and 568 nm, respectively, both could be ascribed to the inorganic semiconducting moieties $[SbI_6]$[34-36].

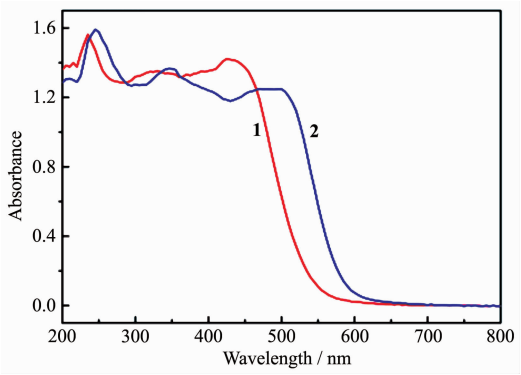

Fig.6 UV-Vis spectra of compounds **1** and **2** in solid states

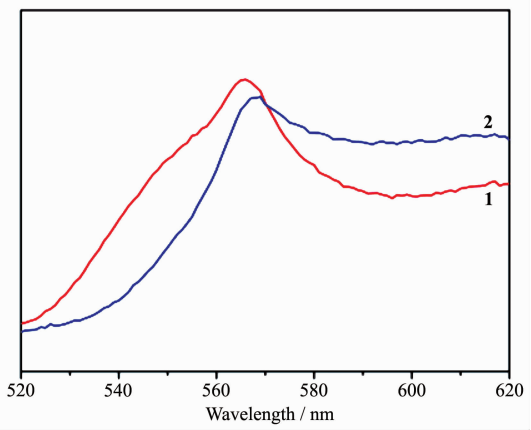

Fig.7 Emission spectra of compounds **1** and **2** in solid states

2.4 DFT calculations

The energy difference between the two configurations of free 1,2-DAC is about 22 kJ·mol^{-1} from DFT calculations, in which the *trans*-configuration is more stable than the *cis*-one. After protonation, the energy difference is little increased to about 28 kJ·mol^{-1}, and configuration conversion was expected between *trans*- and *cis*-configurations. However, compounds **1** and **2** lost their crystalline water at 25~120 ℃ (Fig.2), so it is difficult to discuss the configuration inversion.

3 Conclusions

In this paper, by properly choosing 1,2-cyclohexanediamine (1,2-DAC) with *cis*- and *trans*-configurations to react with semiconductor halide SbI_3, two different organic-inorganic halide (*cis*-1,2-DACH_2)$[SbI_5]\cdot H_2O$ (**1**) and $\{$(*trans*-1,2-DACH_2)$[SbI_5]\cdot H_2O\}_n$ (**2**) were obtained. The single crystal diffraction and DFT calculations revealed that although compounds **1** and **2** are isomers, they are totally different in their properties. The relationship between structure-property is of great significance for further research on the organic-inorganic hybrid materials in practical.

Acknowledgements: We thank the National Natural Science Foundation of China (Grants No.21571094, 21661021, 21865015) and the Jiangxi Provincial Department of Science and Technology (Grant No.20161BAB203073) for financial support.

References:

[1] YUAN Huai-Liang (袁怀亮), LI Jun-Peng (李俊鹏), WANG Ming-Kui(王鸣魁). *Acta Phys. Sin.*(物理学报), **2015**,**64**(3): 038405

[2] Price M B, Butkus J, Jellicoe T C, et al. *Nat. Commun.*, **2015**, **6**:8420

[4] Kerner R A, Rand B P. *J. Phys. Chem. Lett.*, **2018**,**9**:132-137

[5] Love J A, Feuerstein M, Wolff C M, et al. *ACS Appl. Mater. Interfaces*, **2017**,**9**:42011-42019

[6] Choi W, Cho M Y, Konar A, et al. *Adv. Mater.*, **2012**,**24**: 5832-5836

[7] Kirchartz T, Bisquert J, Mora Sero I, et al. *Phys. Chem. Chem. Phys.*, **2015**,**17**:4007-4014

[8] Filippetti A, Caddeo C, Delugas P, et al. *J. Mater. Chem. C*, **2017**,**5**:12758-12768

[9] Manser J S, Christians J A, Kamat P V. *Chem. Rev.*, **2016**, **116**:12956-13008

[10]Feng J, Xiao B. *J. Phy. Chem. C*, **2014**,**118**:19655-19660

[11]Chen K, Barker A J, Morgan F L C, et al. *J. Phys. Chem. Lett.*, **2015**,**6**:153-158

[12]Li B, Chrzanowski M, Zhang Y, et al. *Coord. Chem. Rev.*, **2016**,**307**:106-129

[13]Guo X Y, Huang H L, Ban Y J, et al. *J. Membr. Sci.*, **2015**, **478**:130-139

[14]Yu H, Wei Z H, Hao Y H, et al. *New J. Chem.*, **2017**,**41**: 9586-9589

[15]Kataoka S, Banerjee S, Kawai A, et al. *J. Am. Chem. Soc.*, **2015**,**137**:4158-4163

[16]Longo G, Gil Escrig L, Degen M J, et al. *Chem. Commun.*, **2015**,**51**:7376-7378

[17]Gandeepan P, Cheng C H. *Acc. Chem. Res.*, **2015**,**48**:1194-1206

[18]Eddaoud M, Sava D F, Eubank J F, et al. *Chem. Soc. Rev.*, **2015**,**44**:228-249

[19]Lustig W P, Mukherjee S, Rudd N D, et al. *Chem. Soc. Rev.*, **2017**,**46**:3242-3285

[20]Han S, Zhang J, Sun Z, et al. *Inorg. Chem.*, **2017**,**56**:13078-13085

[21]Hamdi M, Karoui S, Oueslati A, et al. *J. Mol. Struct.*, **2018**, **1154**:516-523

[22]Mkaouar I, Hamdi B, Karaa N, et al. *Polyhedron*, **2015**,**87**: 424-432

[23]Ewing S J, Vaqueiro P. *Inorg. Chem.*, **2014**,**53**:8845-8847

[24]Yamada H, Furusho Y, Yashima E. *J. Am. Chem. Soc.*, **2012**, **134**:7250-7253

[25]YUAN Guo-Jun(袁国军), LIU Guang-Xiang(刘光祥), LIU Shao-Xian(刘少贤), et al. *Chinese J. Inorg. Chem.*(无机化学学报), **2018**,**34**:404-408

[26]YUAN Guo-Jun(袁国军), LIU Guang-Xiang(刘光祥), SHI Chao(时超). *Chinese J. Inorg. Chem.*(无机化学学报), **2017**, **33**:1855-1860

[27]Solomek T, Powers-Riggs N E, Wu Y L, et al. *J. Am. Chem. Soc.*, **2017**,**139**:3348-3351

[28]Sheldrick G M. *Acta Crystallogr. Sect. C: Cryst. Struct. Commun.*, **2015**,**C71**:3-8

[29]Sghaier M O M, Holderna-Natkaniec K, Czarneck P, et al. *Polyhedron*, **2014**,**79**:37-42

[30]Wang Y, Shi C, Han X B. *J. Phys. Chem. C*, **2017**,**121**: 23039-23044

[31]Hebig J C, Kuhn I, Flohre J, et al. *ACS Energy Lett.*, **2016**, **1**:309-314

[32]Mao C Y, Liao W Q, Wang Z X, et al. *Dalton Trans.*, **2016**, **45**:5229-5233

[33]Weclawik M, Gagor A, Jakubas R, et al. *Inorg. Chem. Front.*, **2016**,**3**:1306-1316

[34]Sun Z H, Zeb A, Liu S J, et al. *Angew. Chem. Int. Ed.*, **2016**,**55**:11854-11858

[35]Gao W L, Ma Y M, Zhou Y M, et al. *Mater. Lett.*, **2018**,**216**: 84-87

[36]Mix L T, Carroll E C, Morozov D, et al. *Biochemistry*, **2018**, **57**:1733-1747